Initiated Chemical Vapor Deposition (iCVD) of Poly(alkyl acrylates): An Experimental Study

Kenneth K. S. Lau* and Karen K. Gleason*

Department of Chemical Engineering, Massachusetts Institute of Technology, 77 Massachusetts Avenue, Cambridge, Massachusetts 02139

Received January 23, 2006; Revised Manuscript Received March 9, 2006

ABSTRACT: In a two-part investigation, an experimental study and a kinetic model analysis of the initiated chemical vapor deposition (iCVD) of alkyl acrylate polymers are described. In this first part, an experimental study was performed to look at the effect of process parameters on iCVD polymerization. A homologous series of alkyl acrylates, from ethyl up to hexyl acrylate, were iCVD polymerized. The resulting polymers matched well spectroscopically with those from liquid-phase polymerization, demonstrating that stoichiometric polymers with no observable cross-linking can be achieved in a chemical vapor deposition environment. Deposition rate and molecular weight increased by a factor of over 300 and 60, respectively, when monomer saturated vapor pressure, P_{sat}, was reduced from 42.6 to 0.584 Torr at equal gas pressures, P_M. Over three times increase in deposition rate was observed for ethyl acrylate when substrate temperature was reduced from 29 to 17 °C. These trends are attributed to an increase in P_M/P_{sat} or, equivalently, monomer surface concentration in Henry's law limit at low P_M/P_{sat}. Evidence for adsorption-limited iCVD kinetics came from an apparent negative activation energy of −79.4 kJ/mol obtained experimentally that agreed well with a mathematically derived activation energy of −81.8 kJ/mol equal to twice the heat of desorption in the negative sense. Adsorption measurements found Henry's law limit to be valid and, when fitted to a BET equation, allowed the heat of desorption to be calculated. On the basis of this experimental study, process guidelines were made to define the appropriate parameter space for future iCVD polymerization, with P_M/P_{sat} in the range of 0.4−0.7 recommended as an optimal iCVD window.

Introduction

Polymers films and coatings can be made in a number of ways. Most commonly, polymer solutions or emulsions are applied to surfaces by some form of spraying, dipping, or coating with concomitant evaporation of the solvent.[1] Sometimes, a curing or annealing step after solvent removal is required to improve coating quality. Among dry methods, plasma-enhanced chemical vapor deposition is frequently used to form polymer films.[2] However, plasma polymer compositions can deviate significantly from linear polymer stoichiometries due to extensive cross-linking and loss of chemical functionality during deposition.[3] Recently, initiated chemical vapor deposition (iCVD) has been demonstrated as a way to produce stoichiometric polymers that resemble addition polymers from solution, only without the use of a solvent.[4−8] This method allows for a convenient single-step polymerization-and-coating of planar as well as three-dimensional substrates,[9] exploiting the advantages of CVD (e.g., conformal coating, nanometer scale thickness control, solventless processing), while producing polymers that are identical to those obtained from liquid-phase polymerization. Surprisingly, iCVD can produce a variety of functional polymers in a simple manner, among them, poly(tetrafluoroethylene),[4] poly(glycidyl methacrylate),[5] poly(2-hydroxyethyl methacrylate),[6] poly(methyl methacrylate),[7] and poly(perfluoroalkylethyl methacrylate),[8] using monomer−initiator chemistries that are analogous to liquid-phase free radical polymerization.

Essentially, iCVD involves the vapor-phase delivery of initiator and monomer into a vacuum chamber maintained at a pressure typically between 10^{-1} and 1 Torr, thermal activation of the initiator vapor using filament wires heated to a temperature typically in the range of 200−400 °C, and subsequent polymerization of monomer from activated radicals on a surface that is kept at a much lower temperature, typically less than 50 °C, to promote adsorption. As illustrated in Figure 1, the mechanism of iCVD polymerization is believed to occur through three major steps: (1) thermal decomposition of an initiator in the vapor phase to form primary radicals, (2) diffusion and adsorption of primary radicals and monomer from the vapor phase onto a surface, and (3) polymerization of monomer on the surface via initiation, propagation, and termination events to form a continuous polymer coating. iCVD can be succinctly considered as a free radical polymerization in the bulk yet without the presence of a liquid phase. Yet, it is distinct in that, unlike bulk thermal polymerization, iCVD effectively separates the temperature of initiator decomposition from the temperature of polymerization events (initiation, propagation, and termination). This additional degree of freedom should in principle allow a greater degree of control over processing and resulting coating properties. It also provides greater processing flexibility because a lower substrate temperature could be employed to coat heat-sensitive materials such as plastics, fabrics, and pharmaceutics.

As iCVD represents a relatively new concept for producing polymer films and coatings, much effort is still needed to help understand structure−property−processing relationships. A systematic study was therefore made to examine in greater detail the iCVD polymerization process, using alkyl acrylates as a representative addition polymer system. The results of this study will be presented in two parts. The first part, given in this paper, covers experimental trends on iCVD polymerization of a homologous series of alkyl acrylates. The second part, given in the following paper,[10] describes a kinetic model that was developed, based on the reaction scheme proposed in Figure 1, to gain insight into the mechanisms of iCVD polymerization.

* Corresponding authors. E-mail: klau@mit.edu (K.K.S.L.); kkg@mit.edu (K.K.G.).

10.1021/ma0601619 CCC: $33.50
Published on Web 04/11/2006

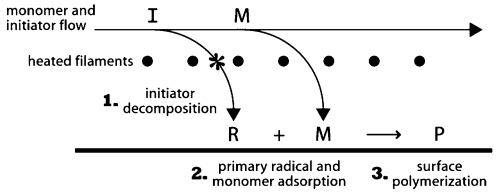

Figure 1. Reaction mechanism proposed for iCVD polymerization. Initiator (I) is thermally decomposed in the vapor phase by heated filaments. Primary radicals (R) and monomer (M) are adsorbed from the vapor phase onto the surface. Polymerization occurs at the surface through radical addition via initiation, propagation, and termination events to form the polymer (P) coating.

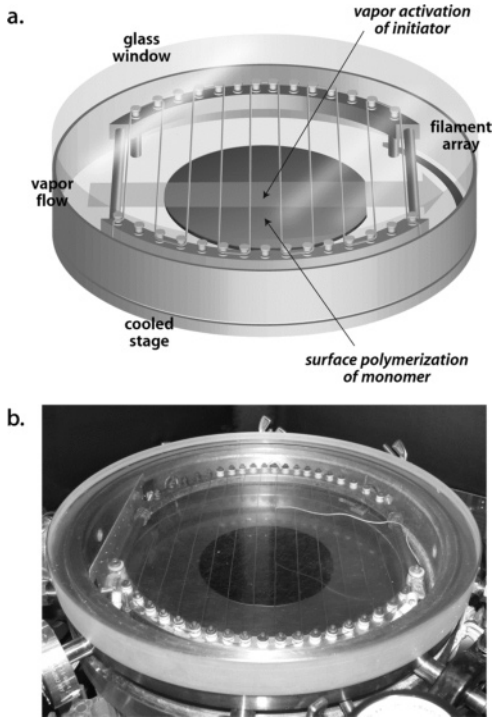

Figure 2. A schematic (a) and photo (b) representation of the iCVD reactor setup for coating on flat substrates. The monomer and initiator flow across an array of heated filaments below which sits the silicon substrate on which the polymer is formed. The substrate is in contact with a stage that is temperature-controlled using recirculating water. The top-side of the reactor consists of a glass window that facilitates real-time monitoring.

Experimental Section

iCVD Polymerization. A homologous series of alkyl acrylate monomers, $CH_2{=}CH(COOR)$, where $R{=}C_nH_{2n+1}$ ($n = 2-6$), with >97% purity, was purchased and used as received without further purification or removal of any inhibitor. Ethyl, *n*-butyl, and *n*-hexyl acrylates were obtained from Aldrich ($n = 2, 4, 6$), while *n*-propyl and *n*-pentyl acrylates were obtained from Scientific Polymer Products ($n = 3, 5$). The radical initiator, *tert*-amyl peroxide $[(C_2H_5)(CH_3)_2CO-]_2$, with 97% purity, was obtained from Aldrich and used as received. Figure 2 shows the setup of the custom-designed iCVD reactor, with internal dimensions of 10 in. diameter and 1.25 in. height, used for deposition on 100-mm-diameter Si (100) substrates. Monomer and initiator vapors were delivered into the reactor by using regulated needle valves through a port on one side of the reactor. For the heavier monomers ($n = 5, 6$), the monomer source vessel was heated to provide sufficient reservoir pressure for vapor delivery. An array of Chromaloy O filaments (Goodfellow), consisting of 14 filaments spaced 1.5 cm apart and suspended over the silicon substrate at a distance of 2.5 cm, was resistively heated to the required filament temperature using a DC power supply (Sorensen). Substrate temperature was controlled by contact with a stage having backside water by using a recirculating chiller/heater (Neslab). Actual substrate temperature was predetermined by using a special silicon wafer with embedded thermocouple sensors (Thermodynamic Sensors), measurements being made at various experimental filament temperature, water temperature, and reactor pressure conditions (using Ar as the "dummy" feed gas) that would mimic actual deposition conditions. Elsewhere, reactor wall temperature was not independently controlled; this temperature, primarily dictated by radiation from the heated filaments, would generally be warmer than the substrate temperature, and given that reactant flow rates and concentrations in this study were adequately high, the influence of chamber wall temperature was considered slight because the walls were not expected to form any limiting reaction sink. Reactor pressure was controlled by using a downstream throttle valve (MKS Instruments) together with a Baratron capacitance manometer (MKS Instruments). Vacuum was achieved by using a roots blower (Leybold) in combination with a dry pump (BOC Edwards) through a pump-out port on the reactor that was positioned on the opposite side to the feed port. During a typical experiment, the silicon wafer was kept at a fixed substrate temperature, monomer and initiator were fed at set flow rates, the system was brought up to pressure, and the filaments were heated to the required temperature. Deposition was monitored in real time by using a He-Ne laser (JDS Uniphase) that reflected off the silicon and growing film, producing an interference laser signal that cycled according to the cycle thickness of the film that was recorded as a function of time.[11]

Thickness Determination. By using spectroscopic ellipsometry, thickness and optical constants of the deposited films were determined. A J. A. Woollam M-2000S equipped with a mapping stage was used to measure the Ψ and Δ angles at 13 points on the coated silicon wafer. Each point measurement was performed at an incidence angle of 70° and for 190 wavelengths between 315 and 718 nm. The raw data was fitted to a model that consisted of a Cauchy−Urbach layer on top of a silicon substrate containing a native oxide surface layer. Convergence allowed the thickness, refractive index, and extinction coefficient to be obtained at each point on the wafer. Film thickness was averaged across all measured points, with uniformity being within 10% (1 SD) of the mean in all cases. Deposition rate was calculated as the ratio of average thickness over deposition time.

Molecular Weight Determination. Molecular weight of the deposited films was determined by using a Waters gel permeation chromatography (GPC) system equipped with an isocratic HPLC pump (model 1515), an in-line degasser (model AF), an autosampler (model 717plus), a Stryagel HR column, and a refractive index detector (model 2414). For each sample, the film was dissolved off of the wafer by using tetrahydrofuran (Aldrich), and the polymer solution adequately concentrated before 100 μL of the solution was injected into the GPC column maintained at 35 °C. The number-average molecular weight and molecular weight distribution were then calculated from the integrated area of the GPC trace, calibrated using a set of narrow poly(methyl methacrylate) standards of known molecular weight and molecular weight distribution.

Compositional Analysis. Fourier transform infrared spectroscopy (FTIR) was used to elucidate the structure and composition of the deposited films. A Thermo Nicolet NEXUS 870 equipped with an MCT-A detector and KBr beam splitter was used in transmission mode to acquire spectra at 4 cm^{-1} resolution over the range of 650−4000 cm^{-1} for 8 scans. Because the FTIR spectra were taken directly of the polymer films on silicon, a background of bare silicon was taken prior to sample acquisition. To compare the structures of iCVD polymer films with counterparts made by using conventional liquid-phase polymerization methods, liquid-phase-polymerized poly(alkyl acrylates) were purchased commercially where available. Poly(ethyl acrylate), poly(*n*-propyl acrylate), poly(*n*-butyl acrylate), and poly(*n*-hexyl acrylate) were obtained from Scientific Polymer Products as polymer solutions in toluene. As poly(*n*-pentyl acrylate) could not be obtained commercially, it was chemically synthesized by bulk polymerization of *n*-pentyl acrylate at 60 °C for 24 h with 0.5 wt % 2,2′-azobisisobutyronitrile (Aldrich) as the radical initiator. The polymer was then placed in a vacuum oven

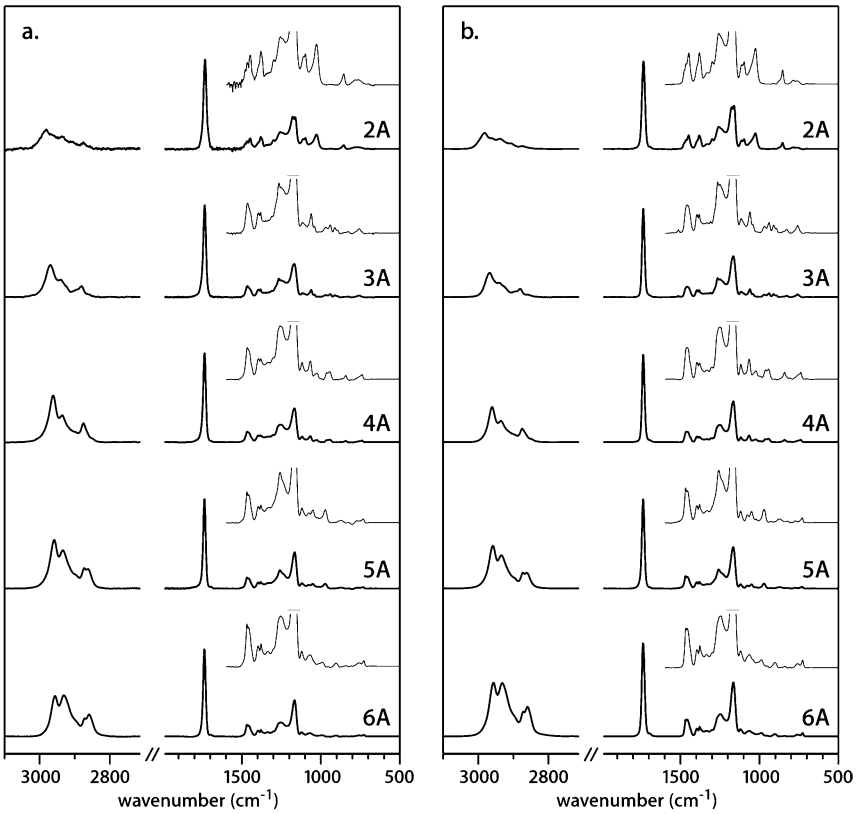

Figure 3. FTIR spectra of a homologous series of poly(alkyl acrylates) made by iCVD (a) and liquid-phase radical polymerization (b). Ethyl (2A), *n*-propyl (3A), *n*-butyl (4A), *n*-pentyl (5A), and *n*-hexyl (6A) acrylate polymers are compared. Insets give vertically expanded spectra within the 1600−500 cm^{-1} region for clearer representation of smaller peaks. The corresponding spectra between each series match well, demonstrating the ability of iCVD to form stoichiometric polymers in a chemical vapor deposition environment. All the spectra show the carbonyl stretch of the ester at ca. 1732−1736 cm^{-1}.

at 100 °C for 24 h to remove any unreacted monomer and subsequently dissolved in tetrahydrofuran. All the polymers derived from liquid-phase polymerization were cast from solution onto silicon prior to FTIR analysis.

Adsorption Measurements. As a way to quantify the concentration of monomer at the surface, adsorption measurements were performed by using a vacuum-compatible Sycon Instruments quartz crystal microbalance (QCM). The setup had a 16-mm-diameter gold-coated crystal sensor that was temperature-controlled by recirculating water from a heater/chiller. In a typical run, the QCM was maintained at a fixed temperature, monomer was then introduced at a fixed flow rate, and pressure was increased to a certain set point. The QCM measured a shift in oscillating frequency of the quartz crystal as a result of adsorption according to the Sauerbrey equation.[12] At equilibrium, the frequency shift was directly related to the mass of monomer adsorbed (in $\mu g/cm^2$). Monomer flow was then switched off, and pressure was allowed to reach back to base pressure. Once again, at equilibrium, the frequency shift in the opposite direction represented the mass of monomer desorbed. The amount of monomer at the surface at a given pressure and substrate temperature was then taken as the average of the adsorption and desorption runs because the monomer only physisorbed on the surface.

Results and Discussion

Polymer Characterization. A homologous series of alkyl acrylates, $CH_2{=}CH(COOR)$, where $R{=}C_nH_{2n+1}$ ($n = 2-6$), was successfully iCVD polymerized and the FTIR spectra of these poly(alkyl acrylates) are shown in Figure 3a. Figure 3b gives the corresponding FTIR spectra of the polymers made from conventional liquid-phase polymerization. The FTIR bands between these two sets of polymers match well, demonstrating iCVD's ability to produce coatings of a wide range of exceptionally clean and well-defined homopolymers under a chemical vapor deposition environment. The carbonyl stretch characteristic of the acrylic ester is observed between 1732 and 1736 cm^{-1}, the peak wavenumber increasing slightly with a longer alkyl pendant group, which is borne out in both series of spectra. Other peaks characteristic of polyacrylic esters at ca. 1250 and 1160 cm^{-1} are also evident in the spectra. As expected, with a longer alkyl side group, the CH_2 peaks at ca. 2935 and 2859 cm^{-1} become more prominent. It is interesting to note that each poly(alkyl acrylate) possesses its own distinctive band features that distinguishes it from the others. For example, the poly(ethyl acrylate) spectrum shows a sharp band at ca. 853 cm^{-1} and a unique splitting of the band at ca. 1160 cm^{-1} into two peaks, while poly(butyl acrylate) can be identified by a double band feature at ca. 950 cm^{-1}.[13]

Effect of Monomer Concentration. The above series of iCVD poly(alkyl acrylates) was deposited at the said process conditions: $F_{monomer} = 3.0$ sccm, $F_{initiator} = 0.7$ sccm, $P_{reactor} = 0.3$ Torr, $T_{filament} = 260$ °C, and $T_{substrate} = 27$ °C. Because deposition conditions remained constant with each monomer run, the only variable was the saturated vapor pressure of the homologous series of monomers used. Table 1 shows the variation in monomer-saturated vapor pressure, P_{sat}, and normal boiling point, T_{bp}, for the series of monomers.[14,15] As seen, P_{sat} is significantly reduced with a longer pendant alkyl chain attached to the monomer, i.e., less of the monomer resides in the vapor phase at equilibrium. Intuitively, this means that, with a heavier monomer, more of it gets adsorbed on the surface at equal monomer gas pressures, P_M. Qualitatively, the ratio P_M/P_{sat} can be used as a measure of the amount of monomer adsorbed on the surface because numerous adsorption isotherms,

Table 1. Saturated Vapor Pressure and Normal Boiling Point of Alkyl Acrylate Monomers

monomer	P_{sat} at $T_{substrate} = 27$ °C (Torr)	T_{bp} at $P = 1$ atm (°C)
ethyl acrylate[a]	42.6	100
n-propyl acrylate[b]	16.6	121
n-butyl acrylate[a]	6.16	147
n-pentyl acrylate[b]	1.75	169
n-hexyl acrylate[b]	0.584	192

[a] Data from ref 14. [b] Data from ref 15.

e.g., the Brunauer−Emmett−Teller or BET equation,[16] relate the amount of material adsorbed on the surface to P_M/P_{sat}, these relationships becoming linear at low P_M/P_{sat} ratios (Henry's law limit).[17,18] In the present case, because pressure and flow rates were constant with each alkyl acrylate polymerization, P_M remained unchanged, i.e., gas concentration of the monomer remained constant. Thus, $1/P_{sat}$ can be directly viewed as a measure of monomer surface concentration.

Figure 4 plots the deposition rate, number-average molecular weight, and polydispersity index (PDI) of the resulting series of alkyl acrylate polymers as a function of $1/P_{sat}$. Both deposition rate and molecular weight increase with an increase in $1/P_{sat}$. Deposition rate shows a greater than 300-fold rise when going from ethyl acrylate to hexyl acrylate polymerization. Molecular weight also shows a significant rise from 1000 to 61 000 g/mol. PDI is between 1.3 and 2.2, which is typical of a conventional free radical polymerization mechanism,[19] although no discernible trend can be made. With $1/P_{sat}$ being a measure of monomer surface concentration, the trends shown in Figure 4 implies that it is the monomer concentration *at the surface* (P_M/P_{sat}) that influences the rate and kinetic chain length of iCVD polymerization. In contrast, the trends in Figure 4 cannot be explained simply by using vapor-phase monomer concentration (P_M) because this gas-phase value was held constant for the series of depositions. But this conclusion is not unequivocal, as differences in rate coefficients of initiation, propagation, and termination reactions across the series of alkyl acrylates could also have influenced the observed kinetics. Although there is a lack of rate data for iCVD polymerization, literature data for liquid-phase radical polymerization of some of these monomers indicate that the propagation constants do not vary significantly in this family of acrylates, with a change of less than a factor of 2 between methyl acrylate ($n = 1$) and dodecyl acrylate ($n = 12$).[20] This means monomer surface concentration may in fact be the more important rate-determining parameter in iCVD.

Effect of Substrate Temperature. To explore the influence of surface concentration further, a series of depositions were made to investigate the effect of substrate temperature on iCVD polymerization of ethyl acrylate. Using a single monomer source would preclude rate effects due to differences in monomer chemistries. Changing substrate temperature would determine if monomer surface concentration were indeed a significant rate determinant. Because a *lower* surface temperature usually leads to greater monomer adsorption, iCVD kinetics should be enhanced if this were the case. On the other hand, if the initiation, propagation, and termination processes were dominant, iCVD kinetics should be enhanced by a *higher* surface temperature because rate coefficients of these events generally follow the usual Arrhenius dependence. iCVD polymerization of ethyl acrylate was performed at the said process conditions: $F_{monomer} = 50.0$ sccm, $F_{initiator} = 1.0$ sccm, $P_{reactor} = 0.75$ Torr, and $T_{substrate} = [17, 21, 25, 29$ °C]. Each set of depositions was carried out at three filament temperatures: $T_{filament} = [285, 310, 360$ °C].

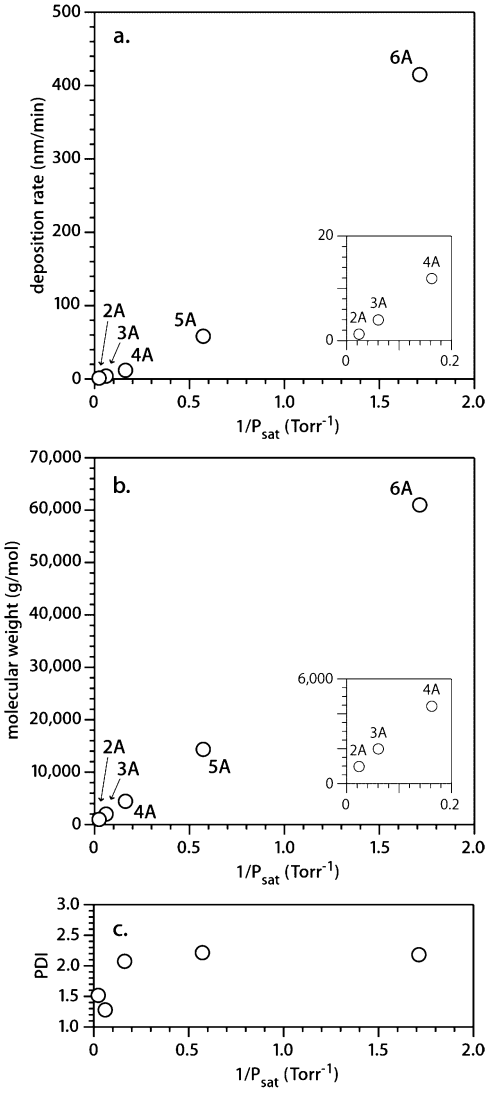

Figure 4. Effect of monomer-saturated vapor pressure on polymer deposition rate (a), number-average molecular weight (b), and polydispersity index (c) in the iCVD of a homologous series of alkyl acrylates. Ethyl (2A), *n*-propyl (3A), *n*-butyl (4A), *n*-pentyl (5A), and *n*-hexyl (6A) acrylate data are shown. Insets in (a) and (b) provide a clearer representation of the data at low $1/P_{sat}$. The effect on deposition rate and molecular weight is strongly dependent on $1/P_{sat}$, which is a measure of monomer surface concentration. On using a heavier monomer (see Table 1) with deposition conditions unchanged, there is a significant increase in kinetics. This is likely due to more favorable monomer adsorption.

Figure 5a shows an Arrhenius plot of the resulting polymer deposition rate as a function of substrate temperature. At each filament temperature, deposition rate increases appreciably with a decrease in surface temperature, strongly indicating that kinetics are adsorption-limited rather than reaction-limited and that monomer surface concentration is most likely the rate-determining factor. Figure 5b, therefore, gives the same deposition rate data but graphed as a function of P_M/P_{sat}, which, as discussed earlier, can be directly related to monomer surface concentration at low P_M/P_{sat} values (less than 0.03 in the present case). This supposition was confirmed with QCM measurements, vide infra.

Interestingly, each of the three sets of data in Figure 5b can be fitted to a curve that is dependent on $(P_M/P_{sat})^2$, i.e., deposition rate (or polymerization rate) is second-order with respect to monomer concentration. This second-order behavior has been similarly observed in liquid-phase free radical polym-

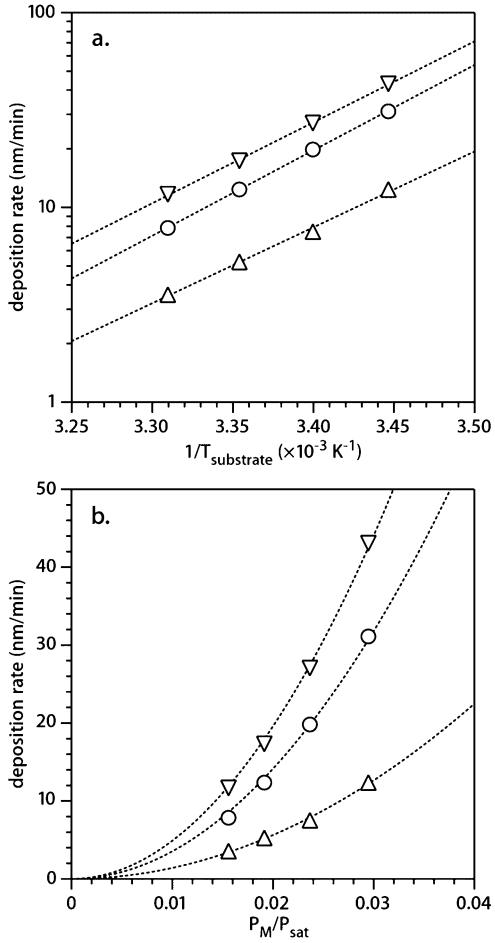

Figure 5. Effect of substrate temperature on polymer deposition rate in the iCVD of ethyl acrylate at filament temperatures of 285 (△), 310 (○), and 360 °C (▽). Plotted as a function of substrate temperature (a), each set of data can be fitted to an Arrhenius form ($R^2 = 0.9959$, 0.9997, and 0.9994, respectively), with a slope that yields an apparent negative activation energy (see Table 2). Plotted as a function of P_M/P_{sat} (b), which is a measure of monomer surface concentration, each set of data can be fitted to a squared dependence on P_M/P_{sat} ($R^2 =$ 0.9957, 0.9993, and 0.9993, respectively), indicating a second-order rate of polymerization. These results point to an adsorption-limited rate process, with a mean activation energy of −79.4 kJ/mol.

erization.[21] Although the rate of polymerization is usually first-order with respect to monomer concentration in liquid-phase radical polymerization, under certain circumstances, the rate may be second-order instead.[19] This can be brought on by a high concentration of primary radicals (radicals formed directly from the decomposition of the initiator) present during polymerization, these radicals being able to terminate growing polymer chains prematurely, leading to a slower polymerization rate.[22] A high primary radical concentration may arise from a high initiator concentration and/or a low monomer concentration so that there is not enough monomer to scavenge off the primary radicals completely or in a suitably quick manner. Presumably, in the present case, conditions were such that there could have been a significant presence of primary radicals on the surface during iCVD polymerization. This is quite probable because depositions were made at fairly low P_M/P_{sat}.

More interestingly, each of the three sets of data in Figure 5a can be regressed to an Arrhenius relationship with a slope that gives an apparent activation energy. Remarkably, the activation energies (or slopes) are close to one another, as given in Table 2. This suggests that the same limiting behavior occurs regardless of filament temperature, with a mean activation

Table 2. Activation Energy of the Arrhenius Relationship between Deposition Rate and Substrate Temperature (at Various Filament Temperatures)[a]

$T_{filament}$ (°C)	E_a (kJ/mol)
285	−74.6
310	−83.9
360	−79.6
	$E_{a,mean} = -79.4 \pm 4.7$

[a] As shown in Figure 5a.

energy of −79.4 ± 4.7 kJ/mol (1 SD). To understand the meaning behind this negative activation energy, an Arrhenius relationship between deposition rate (or polymerization rate) and substrate temperature needs to be derived mathematically. As a first step, monomer surface concentration can be expressed through the limiting form of the BET equation:[23]

$$V_{ad} = \frac{V_{ml}c(P_M/P_{sat})}{(1 - P_M/P_{sat})[1 - (1 - c)(P_M/P_{sat})]}$$

$$c \approx \exp[(\Delta H_{des} - \Delta H_{vap})/(RT)] \qquad (1)$$

$$[M] \sim V_{ad}|_{P_M/P_{sat}\to 0} = V_{ml}c(P_M/P_{sat})$$

where V_{ad} is the total adsorbed volume, V_{ml} is the monolayer adsorbed volume, ΔH_{des} is the heat of desorption, and ΔH_{vap} is the heat of vaporization. Second, P_{sat} can be written in terms of the Clausius−Clapeyron equation:[24]

$$P_{sat} = A \exp[-\Delta H_{vap}/(RT)] \qquad (2)$$

Combining eqs 1 and 2 yields an expression for monomer surface concentration as a function of substrate temperature:

$$[M] \sim \exp[\Delta H_{des}/(RT)] \qquad (3)$$

Finally, with a second-order dependence of deposition rate on monomer surface concentration as determined from Figure 5b,[25] an Arrhenius form relating deposition rate to substrate temperature can be written:

$$\text{rate} \sim [M]^2 \sim \exp[2\Delta H_{des}/(RT)]$$

$$\ln(\text{rate}) \sim 2\Delta H_{des}/(RT) \qquad (4)$$

$$E_a = -2\Delta H_{des}$$

A numerical value for this mathematically derived activation energy can be obtained if ΔH_{des} is known. Through a separate QCM adsorption experiment, which measured the amount of ethyl acrylate monomer adsorbed at various P_M/P_{sat} ratios, the QCM data can be fitted to a BET equation to give a value of c, which can then be used to determine ΔH_{des}, as outlined by eq 1. Figure 6 plots the QCM data as the adsorbed volume, V_{ad}, which was converted from the raw data in μg/cm^2 by using the liquid density of ethyl acrylate and QCM sensor area.[26] Figure 6 also provides the corresponding areal concentration, N_s, in molecules/cm^2, derived from the raw data by using the molar mass of ethyl acrylate. Fitting yields V_{ml} and c of 292.6 pL and 1.950, respectively, which corresponds to an areal concentration for a monolayer of 8.01×10^{14} cm^{-2} at P_M/P_{sat} of 0.417. Taking a literature ΔH_{vap} of 39.2 kJ/mol,[14] ΔH_{des} is calculated as 40.9 kJ/mol. This is within the range of physisorption enthalpies (20−80 kJ/mol) for small molecules that interact with surfaces through van der Waals forces.[27] From eq 4, E_a is then estimated to be −81.8 kJ/mol, which compares well with the experimental E_a of −79.4 kJ/mol derived from the slopes of the Arrhenius

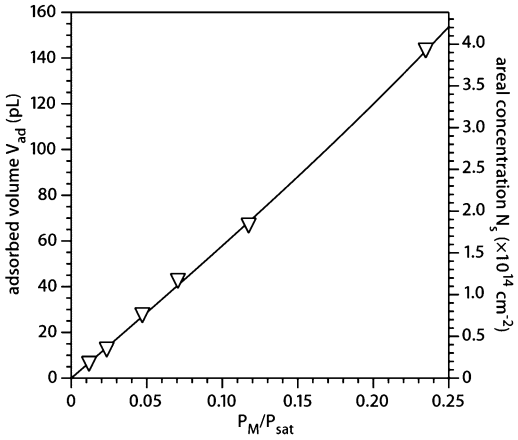

Figure 6. QCM measurements of ethyl acrylate adsorption at 27 °C. The raw data was converted from μg/cm^2 to adsorbed volume, V_{ad}, in pL using the liquid density of ethyl acrylate (0.914 g/cm^3) and QCM sensor area (2.011 cm^2), and also converted to a real concentration, N_s, in molecules/cm^2 using the molar mass of ethyl acrylate (100 g/mol). The data can be fitted to a BET equation ($R^2 = 0.9994$), from which the values of the fitted parameters V_{ml} and c are 292.6 pL and 1.950, respectively, corresponding to a monolayer areal concentration of 8.01 $\times$ 10^{14} cm^{-2} at P_M/P_{sat} of 0.417. A heat of desorption is calculated as 40.9 kJ/mol, which can be related to an activation energy, $E_a = -2\Delta H_{des}$, i.e., -81.8 kJ/mol, with substrate temperature that agrees well with the experimental value from Figure 5.

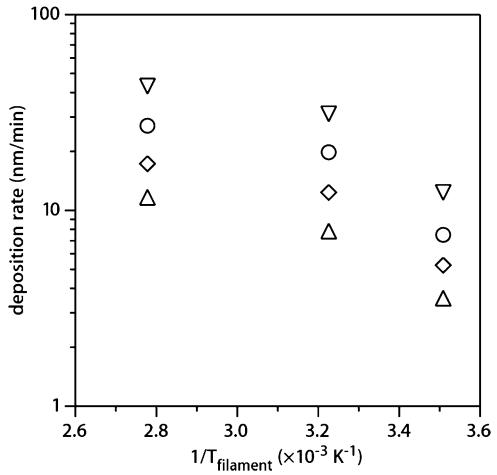

Figure 7. Effect of filament temperature on polymer deposition rate in the iCVD of ethyl acrylate at substrate temperatures of 17 (▽), 21 (○), 25 (◇), and 29 °C (△). Plotted in Arrhenius form, rate increases with filament temperature.

plots in Figure 5a. This agreement lends further credible support that iCVD polymerization kinetics are adsorption-limited and governed predominantly by the monomer concentration at the surface, at least within the range of process conditions used here, although similar adsorption-limited behavior has been reported in iCVD polymerization of other polymer systems and at higher monomer concentrations.[28]

Effect of Filament Temperature. For ethyl acrylate iCVD polymerization, deposition rate data in Figure 5a can be replotted as a function of filament temperature. As shown in Figure 7, there is an increase in rate as filament temperature increased. This increase, however, is modest relative to the temperature dependence of the gas-phase decomposition of the *tert*-amyl peroxide initiator, which has an activation energy of ~155 kJ/mol.[29,30] Hence, the kinetics of initiator decomposition are unlikely to be rate limiting at these conditions. Further quantitative analysis is complicated by the gas-phase temperature gradient around each filament that is determined by its interaction with cold surfaces and other surrounding hot filaments. Such temperature gradients impact both the initiator decomposition rate and the mass transfer rate of primary radicals from the region near the filament to the deposition surface. Further work, beyond the scope of this report, needs to be done to determine the temperature profile in the gas phase and to evaluate its impact on iCVD kinetics. Additionally, it is important to note that initiator-to-monomer feed ratios of 0.1−1.0 used in iCVD experiments are significantly higher than the ratios of less than 0.01 typically found in liquid-phase radical polymerization.[31] This implies that initiator concentration is most likely in excess under these iCVD conditions. Indeed, previous studies have shown that iCVD rates can become independent of initiator concentration.[5]

Guidelines for iCVD Polymerization. The study brings to light certain rules of thumb when performing iCVD polymerization that would be helpful, especially when considering new chemistries and for process optimization. In general, a monomer with a lower saturated vapor pressure, i.e., that is more adsorbing, would tend to yield a faster deposition rate. On the other hand, the choice is constrained by the need to have sufficient vapor pressure to deliver the monomer into the reactor. Although propagation and termination rate processes do not seem to be rate limiting, they nevertheless are expected to influence the rate of polymerization, so monomers with a higher propagation rate coefficient would likely produce faster kinetics. Besides monomer consideration, substrate temperature is a crucial process parameter that requires careful attention. In general, a lower substrate temperature enhances monomer adsorption and would lead to a higher deposition rate. However, there is a lower limit to this temperature, $T_{substrate} = T_{sat}$, at which $P_M = P_{sat}$, because this represents the condensation point of the monomer. Ideal iCVD conditions would, however, be below this limit because a P_M/P_{sat} approaching unity would cause an excess of monomer to arrive at the surface, resulting in the formation of condensation spots, which would in turn yield a low quality, nonuniform deposition. Conversely, too low a P_M/P_{sat} would lead to a reaction-controlled regime that is limited by the amount of monomer on the surface, which would in effect translate to a poor deposition rate. It is recommended that P_M/P_{sat} be in a range such that there would be 1−3 monolayers of monomer at the surface to provide sufficient and yet not an excess of monomer for a suitably fast deposition rate, which, for the case of ethyl acrylate, would be a P_M/P_{sat} range of around 0.4−0.7. Overall, iCVD polymerization is favorable when conditions provide a sufficient amount of monomer on the surface and with sufficient reactivity.

Conclusion

A homologous series of alkyl acrylate monomers, from ethyl up to hexyl acrylate, were iCVD polymerized in a systematic study to examine the iCVD process in more detail. Spectroscopically, the series of iCVD poly(alkyl acrylates) matched well with those from liquid-phase polymerization, showing these iCVD polymers are well-defined and stoichiometric in composition. Monomer-saturated vapor pressure is found to significantly affect iCVD kinetics, with a heavier monomer yielding a higher polymer deposition rate and molecular weight. A less volatile monomer is thought to lead to greater monomer adsorption and a higher monomer concentration at the surface at equal monomer gas concentrations. Substrate temperature is also found to significantly influence iCVD kinetics, with a lower surface temperature yielding a faster polymerization rate. This again is attributed to a higher monomer surface concentration because adsorption is expected to be enhanced at lower substrate

temperatures. An apparent negative activation energy based on an Arrhenius relation between deposition rate and substrate temperature is observed. This compared well with a mathematically derived activation energy that is equal to twice the heat of desorption (negative sense), having based this on an observed second-order rate with respect to P_M/P_{sat}, which, in the Henry's law limit, is a linear measure of monomer surface concentration. QCM adsorption measurements fitted to a BET equation validated this claim and allowed a heat of desorption to be calculated. The good agreement in the activation energies provided quantitative evidence for an adsorption-limited iCVD rate process. Although a higher filament temperature also produced a higher deposition rate, the effect is much less compared with that of substrate temperature. This paper has concentrated on understanding the effect of process parameters on iCVD polymerization through an experimental study, which proved useful in forming guiding principles for selecting appropriate iCVD chemistries and process conditions. It also highlighted the interesting nature of iCVD in requiring a lower surface temperature for more favorable polymerization, this unique property making the coating of temperature-sensitive substrates, e.g., plastics, fabrics, and pharmaceutics, realizable. In the following paper, focus will shift to the development of a kinetic model for iCVD polymerization in an attempt to express more explicitly the reaction mechanisms that could be underlying this process.

Acknowledgment. We thank the DuPont MIT Alliance for financial support. We especially thank Dr. John H. McMinn of DuPont Central Research & Development for helpful discussions.

References and Notes

(1) Slone, R. V. In *Encyclopedia of Polymer Science and Technology*, 3rd ed.; Kroschwitz, J. I., Mark, H. F., Eds.; John Wiley & Sons: Hoboken, NJ, 2003; Vol. 1, pp 96−124.
(2) Yasuda, H. In *Plasma Polymerization*; Academic Press: Orlando, FL, 1985.
(3) d'Agostino, R.; Cramarossa, F.; Fracassi, F.; Illuzzi, F. In *Plasma Deposition, Treatment, and Etching of Polymers*; d'Agostino, R., Ed.; Academic Press: San Diego, CA, 1990; p 147.
(4) Lau, K. K. S.; Bico, J.; Teo, K. B. K.; Chhowalla, M.; Amaratunga, G. A. J.; Milne, W. I.; McKinley, G. H.; Gleason, K. K. *Nano Lett.* **2003**, *3*, 1701−1705.
(5) Mao, Y.; Gleason, K. K. *Langmuir* **2004**, *20*, 2484−2488.
(6) Chan, K.; Gleason, K. K. *Langmuir* **2005**, *21*, 8930−8939.
(7) Chan, K.; Gleason, K. K. *Chem. Vap. Deposition* **2005**, *11*, 437−443.
(8) Ma, M.; Mao, Y.; Gupta, M.; Gleason, K. K.; Rutledge, G. C. *Macromolecules* **2005**, *38*, 9742−9748.
(9) Lau, K. K. S.; Gleason, K. K. *J. Am. Chem. Soc.*, submitted.
(10) Lau, K. K. S.; Gleason, K. K. *Macromolecules* **2006**, *39*, 3695−3703.
(11) Cruden, B.; Chu, K.; Gleason, K.; Sawin, H. *J. Electrochem. Soc.* **1999**, *146*, 4590−4596.
(12) Sauerbrey, G. *Z. Phys.* **1959**, *155*, 206−222.
(13) Hummel, D. O.; Scholl, A. S. In *Atlas of Polymer and Plastics Analysis*; Carl Hanser Verlag: Munich, 1988; Vol. 2, p 374.
(14) Afeefy, H. Y.; Liebman, J. F.; Stein, S. E. In *NIST Chemistry WebBook, NIST Standard Reference Database, Number 69*; Linstrom, P. J., Mallard, W. G., Eds.; National Institute of Standards and Technology: Gaithersburg, MD, 2005; http://webbook.nist.gov.
(15) Obtained from SciFinder Scholar 2006 (Chemical Abstracts Service, American Chemical Society: Columbus, OH). Estimated through group contribution methods using ACD/Labs Software version 8.14 for Solaris (Advanced Chemistry Development: Toronto, Canada)
(16) Brunauer, S.; Emmett, P. H.; Teller, E. *J. Am. Chem. Soc.* **1938**, *60*, 309−319.
(17) Beach, W. F. *Macromolecules* **1978**, *11*, 72−76.
(18) Flory, P. J. In *Principles of Polymer Chemistry*; Cornell University Press: Ithaca, NY, 1953; p 514.
(19) Odian, G. In *Principles of Polymerization*, 4th ed.; John Wiley & Sons: Hoboken, NJ, 2004; pp 198−349.
(20) Asua, J. M.; Beuermann, S.; Buback, M.; Castignolles, P.; Charleux, B.; Gilbert, R. G.; Hutchinson, R. A.; Leiza, J. R.; Nikitin, A. N.; Vairon, J.-P.; van Herk, A. M. *Macromol. Chem. Phys.* **2004**, *205*, 2151−2160.
(21) Yoshioka, M.; Otsu, T. *Macromolecules* **1992**, *25*, 559−562.
(22) Lebreton, P.; Boutevin, B. *J. Polym. Sci., Part A: Polym. Chem.* **2000**, *38*, 1834−1843.
(23) Adamson, A. W.; Gast, A. P. In *Physical Chemistry of Surfaces*, 6th ed.; John Wiley & Sons: New York, 1997; pp 618−620.
(24) Atkins, P.; de Paula, J. In *Physical Chemistry*, 7th ed.; W. H. Freeman & Co.: New York, 2002; p 147.
(25) Although Figure 5b relates P_M/P_{sat} to monomer surface concentration, strictly speaking, based on the BET equation, $c(P_M/P_{sat})$ should be used because c is also dependent on substrate temperature. However, in this particular case, c is relatively insensitive to substrate temperature compared to P_{sat} due to a small value of $(\Delta H_{des} - \Delta H_{vap})$. Further, other limiting forms of monomer surface concentration do not include this additional factor. Even if c were included, this did not alter the order of the rate of polymerization derived through Figure 5b.
(26) Karpovich, D. S.; Blanchard, G. J. *Langmuir* **1997**, *13*, 4031−4037.
(27) Hayword, D. O.; Trapnell, B. M. W. In *Chemisorption*, 2nd ed.; Butterworth: London, 1964; p 198.
(28) Chan, K.; Gleason, K. K. *Macromolecules*, accepted.
(29) Perona, M. J.; Golden, D. M. *Int. J. Chem. Kinet.* **1973**, *5*, 55−65.
(30) Raley, J. H.; Rust, F. F.; Vaughan, W. E. *J. Am. Chem. Soc.* **1948**, *70*, 88−94.
(31) Braun, D.; Cherdron, H.; Rehahn, M.; Ritter, H.; Volt, B. *Polymer Synthesis: Theory and Practice. Fundamentals, Methods, Experiments*; Springer: New York, 2005.

MA0601619